A Thermal Conductivity Model for CNT-Polymer Composites Considering Curvature, Orientation, and Interfacial Resistance

Xuanyi Yang（杨烜屹）[1†], Zengqiang Cao（曹增强）[2†], Zhejun Xiang（向哲俊）[3], Xin Huang（黄鑫）[4], Yanqing Wang（王延青）[5], Chaoyang Zhang（张朝阳）[4,6], Yuxiang Ni（倪宇翔）[1*]

[1] School of Physical Science and Technology, Southwest Jiaotong University, Chengdu 610031, China

[2] Department of Forensic Science and Technology, Zhengzhou Police University, Zhengzhou 450053, China

[3] Department of Mathematical Engineering, Faculty of Engineering, Musashino University, Tokyo 135-8181, Japan

[4] Institute of Chemical Materials, China Academy of Engineering Physics (CAEP), P.O. Box 919-311, Mianyang 621900, China

[5] College of Polymer Science and Engineering, State Key Laboratory of Advanced Polymer Materials, Sichuan University, Chengdu 610065, China

[6] Beijing Computational Science Research Center, Beijing 100048, China

[†]These authors contributed equally to this work.

*Corresponding author. E-mail address: yuxiang.ni@swjtu.edu.cn (Y. Ni).

Abstract

A theoretical model is proposed to predict the effective thermal conductivity of CNT–polymer composites by coupling interfacial thermal resistance, CNT waviness, orientation, and aggregation effects. A stepwise-discrete angle and equivalent length method are used to characterize heat flux loss in curved CNTs. The model is validated against experimental data and compared with the Hasselman–Johnson and Deng models. Results show that the present model greatly improves prediction accuracy and effectively avoids overestimation under low and moderate loadings. This work provides

a reliable theoretical approach for the design and optimization of high-performance thermally conductive composites in electronic packaging and aerospace applications.

Keywords: Theoretical model, thermal conductivity, CNT–polymer composites, interfacial thermal resistance,

PACS: 65.80.-g, 44.10.+i, 66.70.Lm, 81.05.Qk, 44.05.+e

1. Introduction

With the growing demand for efficient thermal management in aerospace, automotive manufacturing, and electronic packaging, thermally conductive polymer composites show broad application prospects due to their light weight, ease of processing, and low cost[1-3]. However, their thermal transport properties are governed by complex, coupled effects of filler type, interfacial structure, and microstructural distribution, which are difficult to fully elucidate through experimental approaches alone[4-6]. Therefore, developing theoretical models that quantitatively link microstructural characteristics to macroscopic thermal conductivity is essential for material optimization.

Traditional thermal conductivity models, while effective for conventional filler systems, face significant challenges when applied to low-dimensional nanomaterials such as carbon nanotubes (CNTs). CNTs possess extremely high intrinsic thermal conductivity and excellent mechanical properties, making them highly promising thermal enhancement fillers[7, 8]. However, in practical applications, CNTs are prone to bending, entanglement, and agglomeration, with factors such as dispersion state, orientation distribution, and interfacial thermal resistance significantly influencing heat conduction[9-11]. These complex microstructural characteristics often lead to substantial discrepancies between experimental measurements and theoretical predictions.

For example, the model proposed by Deng et al. indicates that high-aspect-ratio CNTs can significantly enhance composite thermal conductivity[12]. However, this model employs an idealized treatment for curved CNTs, neglecting heat flux losses due to geometric tortuosity, and thus often overestimates their thermal contribution—

particularly under low loading conditions where predictive accuracy is critical. Similarly, Xue proposed a thermal conductivity model for CNT-reinforced composites that incorporates corrections for interfacial thermal resistance. However, this model is still based on the idealized assumption of perfectly straight CNTs, neglecting the commonly observed waviness of CNTs in practical matrices. Such geometric simplification often leads to an overestimation of the effective aspect ratio of the fillers, resulting in theoretical predictions that exceed the experimental measurements[13]. In light of these findings, Huang et al. introduced nonlinear correction terms related to percolation theory within the effective medium theory (EMT) framework, accounting for CNT entanglement and dispersion states, in order to fit the nonlinear trends observed in experiments at high filler concentrations[14]. Although this approach improves the agreement between the model and experimental results to some extent, it remains essentially an empirical correction, as it reduces the complex behaviors of CNT dispersion and agglomeration to a single exponential parameter, cannot accurately capture the thermal transport behavior of the actual microstructure.

To address these limitations, this study develops a micromechanics-based model that (i) incorporates interfacial thermal resistance via the Kapitza resistance layer, (ii) accounts for CNT curvature by projecting local heat flux onto the primary temperature gradient, and (iii) introduces a uniformity factor to quantify dispersion effects. Using this model, we quantitatively analyze the effects of CNT loading, orientation distribution, and interfacial thermal resistance on composite thermal conductivity, validating the model's accuracy against experimental data. The results provide a theoretical basis for designing high-performance CNT-reinforced composites and offer new insights for predicting thermal conductivity in low-loading CNT systems.

2. Theoretical Model

The thermal conductivity of carbon nanotube (CNT)-reinforced polymer nanocomposites, especially for low-loading composites with randomly oriented, high

aspect ratio, straight CNTs of average length L and diameter d, can be estimated using the initial form of the model proposed by Deng et al[12].

$$\frac{k_e}{k_m} = 1 + \frac{f/3}{k_m / k_{33}^c + H} \tag{1}$$

In the equation, f represents the volume fraction of CNTs, k_{33}^c denotes the axial thermal conductivity of CNTs, k_m is the thermal conductivity of the isotropic matrix, and k_e stands for the effective thermal conductivity of the CNT composite material. The term H in the expression accounts for the influence of the aspect ratio P=L/d, where L and d are the length and diameter of the CNTs, respectively.

$$H(p) = \frac{1}{(p)^2 - 1}\left[\frac{p}{\sqrt{(p)^2 - 1}} \ln\left(p + \sqrt{(p)^2 - 1}\right)\right] \tag{2}$$

To capture the impact of interfacial thermal resistance on the effective thermal conductivity of the CNT/polymer composite, a Kapitza interfacial thermal resistance layer is applied to straight CNTs, as shown in Figure 1[11, 15].

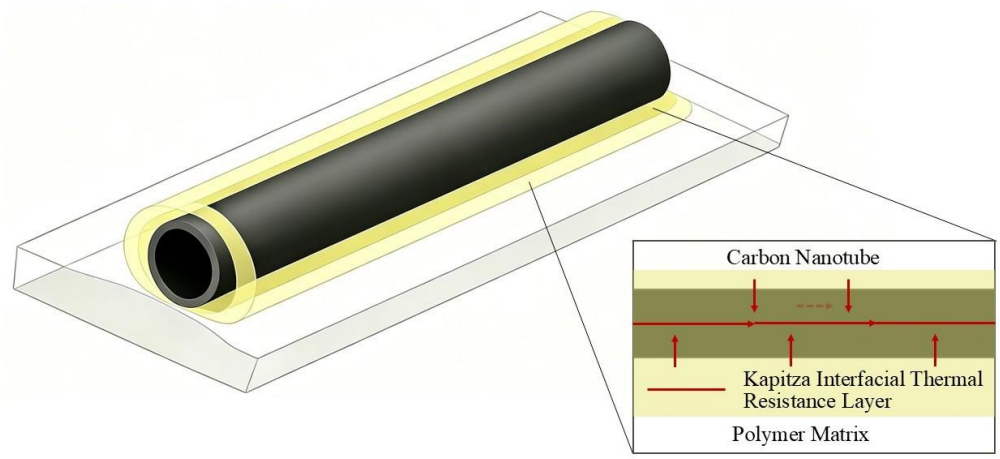


Fig. 1. Schematic of a Carbon Nanotube Coated with a Kapitza Interfacial Thermal Resistance Layer.

Assume a heat flow Q is transmitted from one end of the carbon nanotube (CNT) to the other. In this process, the heat flow needs to pass through both the intrinsic thermal conductivity of the CNT and the interfacial resistance layers on both sides. The interfacial thermal resistance causes a temperature jump at the interface between the CNT and the surrounding matrix. The intrinsic axial thermal conductivity of the CNT

is denoted by k_{33}^{c}, and after applying the Kapitza interfacial thermal resistance layer, the effective axial thermal conductivity of the CNT becomes k_{33}^{cr}.

In the following equations, we denote L the length of the CNT, A the cross-sectional area of the CNT, q the heat flux density through the CNT, and R_k the interfacial thermal resistance. Without considering the effect of interfacial thermal resistance R_k, the heat flux through the CNT can be expressed as:

$$Q = k_{33}^{c} \cdot A \cdot \frac{\Delta T}{L} \tag{3}$$

Considering the effect of interfacial thermal resistance R_k, and each CNT is connected to the surrounding matrix through two interfaces, the heat flux through the CNT can be expressed as:

$$Q = k_{33}^{cr} \cdot A \cdot \frac{\Delta T - 2 \cdot q \cdot R_k}{L} \tag{4}$$

By combining Eq. (3) and (4), Eq. (5) can be obtained:

$$k_{33}^{cr} = k_{33}^{c} / (1 + 2R_k \cdot k_{33}^{c} / L) \tag{5}$$

Now we have the expression of k_{33}^{cr}, the equivalent axial thermal conductivity of CNTs encapsulated by interfacial thermal resistance layers. This allows us to make model predictions that account for interfacial thermal resistance R_k:

$$\frac{k_e}{k_m} = 1 + \frac{f/3}{k_m / k_{33}^{cr} + H} \tag{6}$$

From a microscopic perspective, carbon CNTs within the composite typically exhibit a curved or non-straight configuration due to their high aspect ratio, as shown in Figure 2. This curved geometry impacts their thermal conduction capability. To accurately describe the heat transfer mechanism of CNTs in the composite, this study focuses on the influence of the axial thermal conductivity of CNTs and the heat flux density along their orientation.

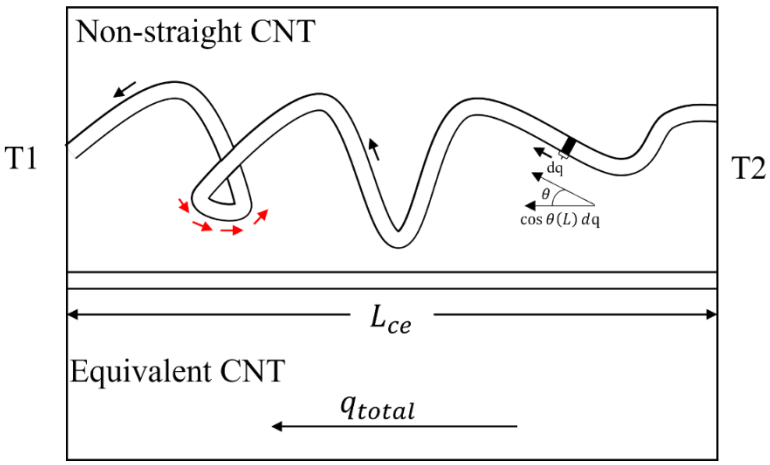


Fig. 2. Schematic Diagram of the Heat Conduction Process in a Non-straight CNT.

Non-straight CNTs exhibit more complex thermal conduction behavior, particularly at bends or loops (e.g., the areas marked with red arrows in Fig. 2). In these local curved regions, the direction of heat flux can deviate significantly and may even reverse. Therefore, accurately approximating the overall heat distribution requires careful consideration of the geometry of individual CNT sections and their orientation relative to the primary heat flux direction.

Under a temperature difference $\Delta T = T_2 - T_1$, the overall heat flux density q_{total} aligns with the temperature gradient. For a curved CNT, each infinitesimal segment dL conducts heat along its local tangent, forming an angle θ with the primary heat flux direction. The contribution of such a segment to the total heat flux in the primary direction is given by $dq\ cos\ \theta\ (L)$.

By integrating $dq\ cos\ \theta\ (L)$ over the total length L of the non-straight CNT, the effective projection length contributing to macroscopic heat transfer can be quantified. The angle θ is defined piecewise along the CNT length and varies with the bending of the CNT. It characterizes the local deviation between the tangent direction of CNT and the macroscopic temperature gradient direction.

The CNT is divided into finite segments of finite length, and θ is defined piecewise and varies stepwise with CNT bending, rather than varying continuously. The integral of projection terms over the full CNT length is expressed as:

$$\int_0^L \cos\theta(L)\mathrm{d}L = L \cdot \mu \tag{7}$$

where μ denotes the length-averaged orientation factor, which describes the average alignment degree between all CNT segments and the principal heat flow direction; its rigorous mathematical definition will be derived subsequently.

To extract the position-dependent angle $\theta(L)$ required to evaluate Eq. (7) from experimental characterizations, the central skeleton of each CNT is traced from TEM, SEM or 3D nanotomography scans and discretized into a series of coordinate points $\boldsymbol{r}_0$, $\boldsymbol{r}_1$, ..., $\boldsymbol{r}_n$. For the i-th discrete segment, the segment vector and geometric length are defined as

$$\Delta \boldsymbol{r}i = \boldsymbol{r}i + 1 - \boldsymbol{r}_i, \quad \Delta L_i = |\Delta \boldsymbol{r}_i| \tag{8}$$

The cosine value of the angle between the local CNT tangent and the global heat flow unit vector is solved via vector dot product:

$$cos\,\theta_i = \frac{\Delta \boldsymbol{r}_i \cdot \boldsymbol{e}_T}{|\Delta \boldsymbol{r}_i|} \tag{9}$$

In the above expression, $\boldsymbol{e}_T$ denotes the unit vector parallel to the macroscopic temperature gradient (the dominant global heat flow direction inside composites), and its magnitude satisfies $|\boldsymbol{e}_T| = 1$.

The continuous integral in Eq. (7) is replaced by finite summation for numerical implementation:

$$\int_0^L cos\,\theta(L)dL \approx \sum_{i=1}^{n} cos\,\theta_i \Delta L_i \tag{10}$$

For a composite with abundant randomly distributed CNTs, the bulk orientation factor μ is calculated by length-weighted statistics across all segmented elements of all fillers:

$$\mu \approx \frac{\sum_j \sum_i cos\,\theta_{ij} \Delta L_{ij}}{\sum_j L_j} \tag{11}$$

It is worth noting that two-dimensional electron micrographs only record planar projected profiles and underestimate out-of-plane CNT tortuosity, whereas three-dimensional tomographic reconstruction delivers more accurate angular data. For the reference experimental data adopted for model validation in this paper, raw three-dimensional coordinate information of CNTs cannot be accessed. Hence, we derive the lumped equivalent structural parameters by fitting experimental thermal conductivity

data, instead of directly calculating them through segment-by-segment discrete integration from CNT micro-morphology.

Additionally, the curved CNT can be modeled as an equivalent straight CNT (Fig. 2) that transfers the same total heat flux q_{total}, with an effective length L_{ce}. Given the effective axial thermal conductivity of the equivalent straight CNT as k_{33}^{cr}, the heat flux density can be expressed as:

$$q_{total} = \frac{k_{33}^{cr} \Delta T}{L_{ce}} \tag{12}$$

For the actual curved CNT, the total effective heat flux along the macroscopic temperature gradient is obtained by averaging the projected heat contribution over the full curved length:

$$q_{total} = \frac{k_{33}^{cr} \Delta T}{L} \int_0^L cos\,\theta(L) dL \tag{13}$$

By equating the two expressions of q_{total} and canceling the identical terms k_{33}^{cr} and ΔT on both sides, we obtain:

$$\frac{1}{L_{ce}} = \frac{1}{L} \int_0^L cos\,\theta(L) dL \tag{14}$$

We define $\eta = L_{ce}/L$ as the waviness factor, which characterizes the degree of geometric undulation of non-straight CNTs. Its value ranges within [0,1], where $\eta = 1$ corresponds to a perfectly straight CNT, and $\eta \to 0$ indicates a highly tortuous CNT.

The rigorous definition of the orientation factor μ is given as:

$$\mu = \frac{1}{L} \int_0^L cos\,\theta(L) dL \tag{15}$$

μ ranges within [0,1], where $\mu = 1$ indicates that all CNT segments are perfectly parallel to the principal heat flow direction, and $\mu = 0$ indicates perpendicular alignment. Local tangent angles of curved CNTs can be extracted from TEM, SEM or 3D nanotomography images.

During the experimental preparation of CNT-polymer composites, CNTs tend to aggregate, which enhances inter-CNT interactions and significantly reduces the effective thermal conductivity. To quantitatively describe this effect, we introduce an aggregation factor γ into Eq. (15). The aggregation factor γ characterizes the degree of CNT clustering within the matrix, which accounts for the reduction in effective heat

transfer pathways caused by CNT agglomeration. Physically, increasing γ reduces the filler dispersion in the composite, thereby lowering the composite thermal conductivity. The value of γ ranges from 0 (perfectly uniform dispersion) to 1 (complete agglomeration).

Now, the waviness factor η, orientation factor μ and aggregation factor γ are derived separately from the geometric heat flux projection analysis in Eqs. (7)–(15). Compared with the straight-CNT baseline model Eq. (6), η, μ and γ are embedded into the model according to their respective physical effects on heat transport. η globally corrects the effective length and aspect ratio of curved CNTs, while μ and $(1-\gamma)$ jointly reduce the effective axial thermal conductivity of CNTs by accounting for random segment orientation and filler agglomeration. Finally, the comprehensive thermal conductivity model Eq. (16) that simultaneously accounts for curvature, orientation, aggregation and interfacial resistance is established:

$$\frac{k_e}{k_m} = 1 + \frac{\eta f/3}{\frac{k_m}{\mu(1-\gamma)\eta k_{33}^{cr}} + H(\eta P)} \tag{16}$$

3. Results and Discussion

To systematically evaluate the validity and predictive capability of the proposed model, the Halpin-Tsai model (H–T) model[16, 17] and the micromechanical model developed by Deng et al.[12] were selected as benchmark models for comparison. The Halpin-Tsai model is a semi-theoretical framework widely used to estimate the effective thermal conductivity of two-phase composites by incorporating the effects of filler thermal conductivity, volume fraction, geometry, orientation, and packing characteristics through structural parameters. Predictions from the three models were compared with experimental data under consistent parameter settings, enabling a quantitative assessment of their accuracy and reliability. This comparison provides a direct evaluation of the predictive performance of the present model for thermal transport in CNT-based composites. To determine η, μ, and γ values, we fix constant intrinsic parameters unchanged: matrix thermal conductivity □□, intrinsic axial thermal conductivity of CNT □□□□, CNT geometric dimensions (length L,

diameter d), volume fraction f, and interfacial thermal resistance R_{Kp} derived from published typical experimental values. Then, we constrain the values of η, μ, and γ within its physically reasonable range, then adopt nonlinear least-squares fitting to minimize the MSE between model predictions and experimental thermal conductivity data, so as to solve for optimal η, μ, and γ.

3.1 Thermal Conductivity Predictions for Low-Loaded CNT Composites

Model performance was first validated against experimental data for multi-walled carbon nanotubes (MWNTs) dispersed in synthetic oil[18]. The baseline parameters were set as follows: matrix thermal conductivity k_m=0.1448 W/mK, intrinsic CNT thermal conductivity k_{CNT}=2000 W/mK, CNT diameter d=25 nm, and CNT length L=50 μm.

As shown in Figure 3, the H–T model significantly overpredicts the thermal conductivity enhancement at low CNT volume fractions, deviating noticeably from experimental measurements. The model of Deng et al. improves prediction to some extent but still overestimates the composite thermal conductivity, because it neglects heat flux loss caused by CNT curvature and underestimates thermal isolation between adjacent CNTs. In contrast, predictions from the proposed model (Eq. (16)) agree well with experimental data across the entire loading range, demonstrating high accuracy at low filler fractions.

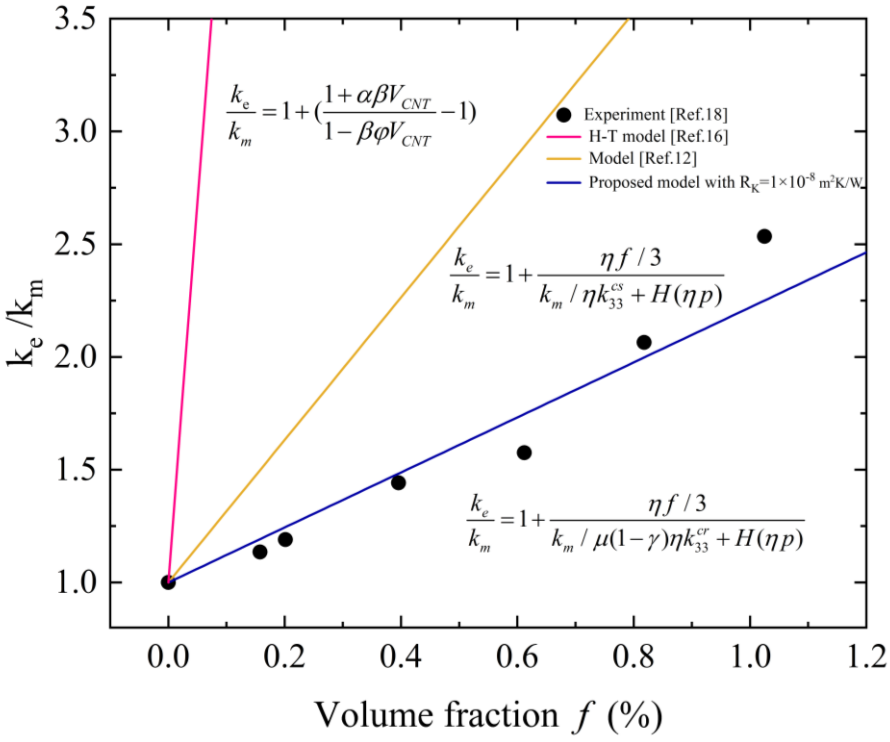


Fig. 3. Thermal conductivity enhancement of low-loading CNT composites: experimental measurements vs predictions from different models. Parameters: waviness factor η = 0.273, orientation factor μ= 0.597, aggregation factor γ= 0.402, k_{33}^{cr} =2000, k_m=0.1448 W/mK, P=2000.

When interfacial thermal resistance $R_k=1\times10^{-8}$ m²K/W is incorporated, the proposed model remains in strong agreement with experiments after slight adjustment of the waviness, orientation, and aggregation factors. This confirms that the model can reliably capture the coupled effects of interfacial thermal resistance, CNT morphology, orientation, and dispersion.

To quantify fitting accuracy, the mean squared error (MSE) was calculated for all three models. The H–T model yields an MSE of 300.35, Deng's model gives 1.34, and the present model achieves an MSE as low as 0.02. These results confirm that the proposed model provides substantially improved accuracy and stability for predicting the thermal conductivity of low-loaded CNT composites.

3.2 Thermal Conductivity Predictions for Moderately-Loaded CNT Composites

The model was further validated using experimental data from oriented MWCNT-reinforced aerospace-grade epoxy composites[19]. Parameters were set as follows: k_m=0.26 W/mK, k_{CNT}=2000 W/mK, d=8 nm, and L=1 mm.

As illustrated in Figure 4, both the H–T model and Deng's model severely overestimate thermal conductivity enhancement, especially at low to moderate volume fractions. By contrast, the proposed model closely follows the experimental trend and accurately reproduces the measured thermal conductivity values. When interfacial thermal resistance is included, the model still maintains excellent agreement with experiments, confirming its flexibility and applicability to realistic composite systems.

The MSE values further support the superiority of the present model: 346022.8 for the H–T model, 29.723 for Deng's model, and only 0.053 for the proposed model. This remarkable improvement in prediction accuracy demonstrates that the model effectively captures the dominant physical mechanisms governing thermal transport, including CNT curvature, orientation distribution, interfacial thermal resistance, and aggregation effects.

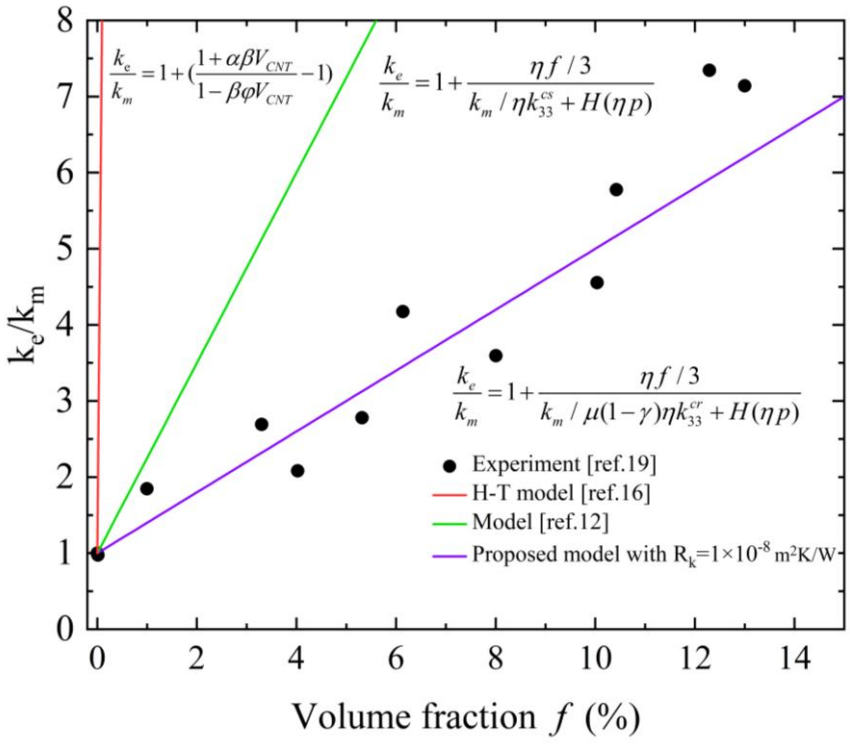


Fig. 4. Thermal conductivity enhancement of moderately loaded CNT composites: experimental measurements vs predictions from different models. Parameters: waviness factor η = 0.22, orientation factor μ= 0.565, aggregation factor γ= 0.434, k_{33}^{cr} =2000, km=0.26 W/mK, P=125000.

3.3 Discussion

The comparative results consistently show that conventional models rely on oversimplified assumptions, such as ideal straight CNTs, neglect of heat flux redirection, and insufficient treatment of CNT–CNT interactions. These limitations lead to systematic over prediction, particularly under low- and moderate-loading conditions.

In contrast, the present model integrates four key factors: (1) Interfacial thermal resistance via the Kapitza resistance layer; (2) CNT waviness using a stepwise-discrete angular distribution and equivalent length; (3) Orientation distribution through an orientation factor; (4) Aggregation effects through an aggregation factor. By accounting for these coupled effects, the model provides physically consistent and highly accurate predictions across diverse CNT–polymer systems. The low MSE values in both datasets confirm that the model is robust, reliable, and suitable for guiding the structural design and performance optimization of the relevant systems.

To quantitatively differentiate the influence strength of the four coupled factors, we can further analyze Eq. (16) and derive analytical sensitivity expressions for each parameter. Orientation factor μ and aggregation factor γ jointly regulate structural thermal resistance with equivalent sensitivity. The waviness factor η exerts complex dual effects by appearing in both the numerator and denominator of the model, introducing multi-path geometric heat loss. A dimensionless parameter Λ is defined to characterize interfacial thermal resistance: when Λ is small, CNT morphology dominates composite thermal conductivity; when $\Lambda \geq 1$, interfacial resistance becomes the primary limiting factor. No fixed priority exists among these four effects, and their relative contributions vary with thermal transport regimes. This hierarchical

coupling mechanism fundamentally accounts for the systematic overestimation of thermal conductivity predicted by conventional ideal straight-CNT models.

It should be noted that the parameters η, μ, and γ can be quantified via SEM/TEM image analysis. For example, η can be obtained by calculating the average ratio of projected straight length to actual curved length of numerous CNTs; μ can be obtained by averaging the cosine of angles between CNT axes and the main heat flow direction; while γ can be obtained by Calibrating with the area fraction of CNT agglomerates from binarized micrographs. In this work, fitting is used to verify the model framework. For follow-up investigations, experimentally measured morphological parameters can be directly imported into the model without fitting. Such morphology-input prediction workflow allows us to accurately evaluate composite thermal conductivity merely from microstructural observations, greatly facilitating the targeted design and performance pre-estimation of thermally conductive CNT-polymer composites.

4. Conclusion

This work developed a comprehensive theoretical model for predicting the effective thermal conductivity of CNT-reinforced polymer composites. The model systematically integrates interfacial thermal resistance, CNT waviness, segment orientation, and aggregation effects to correct the over-simplifications in traditional models, such as ideal straight CNTs, neglected heat flux loss, and insufficient consideration of microstructural non-idealities. By adopting a stepwise-discrete angle description for curved CNTs and introducing an equivalent length method, the model accurately captures the real heat conduction behavior along tortuous CNTs. Comparisons with experimental data and two classical models (Halpin-Tsai and Deng et al.) show that the proposed model significantly improves prediction accuracy, especially under low and moderate CNT loading conditions. The mean squared error (MSE) values are drastically reduced compared with the reference models, verifying the high reliability and stability

of the present model. The validated results confirm that interfacial thermal resistance, CNT curvature, random orientation, and agglomeration jointly suppress the thermal conductivity enhancement, which cannot be ignored in realistic composite systems. The proposed model provides a physically consistent and quantitatively accurate tool for analyzing the thermal transport mechanism of CNT-polymer composites. It can be used to guide the structural design, parameter optimization, and performance prediction of high-performance thermally conductive composites for aerospace, electronic packaging, and advanced thermal management applications.

Acknowledgments

This work was supported by the National Natural Science Foundation of China (NSFC) Grant No. U2330208.

Conflict of interest

The authors declare no conflict of interest.

References

[1] Z. Wang, Z. Wu, L. Weng, S. Ge, D. Jiang, M. Huang, D. M. Mulvihill, Q. Chen, Z. Guo, and A. Jazzar, Adv. Funct. Mater. **33**, 2301549 (2023).

[2] C.-P. Feng, L.-Y. Yang, J. Yang, L. Bai, R.-Y. Bao, Z.-Y. Liu, M.-B. Yang, H.-B. Lan, and W. Yang, Compos. Commun. **22**, 100528 (2020).

[3] K. Ruan, X. Shi, Y. Guo, and J. Gu, Compos. Commun. **22**, 100518 (2020).

[4] Y. Yan, Y. Zhuang, H. Ouyang, J. Hao, and X. Han, Int. J. Heat Mass Transf. **226**, 125445 (2024).

[5] Y. Zhou, S. Wu, Y. Long, P. Zhu, F. Wu, F. Liu, V. Murugadoss, W. Winchester, A. Nautiyal, and Z. Wang, ES Mater. Manuf. **7**, 4-24 (2020).

[6] M. Liu, C. Zhang, Z. Cheng, Z. Liu, L. Chen, and G. Zhao, Mater. Des. **228**, 110788 (2023).

[7] M. Bozlar, D. He, J. Bai, Y. Chalopin, N. Mingo, and S. Volz, Adv. Mater. **22**, 1654-1658 (2010).

[8] M. TabkhPaz, S. Shajari, M. Mahmoodi, D.-Y. Park, H. Suresh, and S. S. Park, Compos. Part B-Eng. **100**, 300-308 (2016).

[9] A. Bagchi and S. Nomura, Compos. Sci. Technol. **66**, 1778-1788 (2006).

[10] D. W. Park and S. E. Shim, Carbon Lett. **11**, 347-356 (2010).

[11] C. W. Nan, X. P. Li, and R. Birringer, J. Am. Ceram. Soc. **83**, 1853-1860 (2000).

[12] F. Deng, Q.-S. Zheng, L.-F. Wang, and C.-W. Nan, Appl. Phys. Lett. **90**, 023107 (2007).

[13] Q. Xue, Nanotechnol. **17**, 1655-1660 (2006).

[14] J. Huang, M. Gao, T. Pan, Y. Zhang, and Y. Lin, Compos. Sci. Technol. **95**, 160-166 (2014).

[15] S. T. Huxtable, D. G. Cahill, S. Shenogin, L. Xue, R. Ozisik, P. Barone, M. Usrey, M. S. Strano, G. Siddons, and M. Shim, Nat. Mater. **2**, 731-734 (2003).

[16] M. Safi, M. Hassanzadeh-Aghdam, and M. Mahmoodi, Polym. Bull. **77**, 4709-4712 (2020).

[17] D. Kumlutas and I. H. Tavman, J Thermoplast. Compos. Mater. **19**, 441-455 (2006).

[18] S. Choi, Z. G. Zhang, W. Yu, F. Lockwood, and E. Grulke, Appl. Phys. Lett. **79**, 2252-2254 (2001).

[19] A. M. Marconnet, N. Yamamoto, M. A. Panzer, B. L. Wardle, and K. E. Goodson, ACS Nano. **5**, 4818-4829 (2011).